

# Reversible Dynamic Optical Sensing Based on Coumarin Modified $\beta$ -Cyclodextrin for Glutathione in Living Cells

Zhixue Liu,<sup>a</sup> Mengdi Tian,<sup>c</sup> Heng Zhang,<sup>c</sup> and Yu Liu<sup>\*ab</sup>

<sup>a</sup> College of Chemistry, State Key Laboratory of Elemento-Organic Chemistry, Nankai University, Tianjin 300071, P. R. China; <sup>b</sup> Haihe Laboratory of Sustainable Chemical Transformations, Tianjin 300192, China; <sup>c</sup> Faculty of Chemical Engineering, Kunming University of Science and Technology, Kunming 650500, Yunnan, China. E-mail: [yuliu@nankai.edu.cn](mailto:yuliu@nankai.edu.cn).

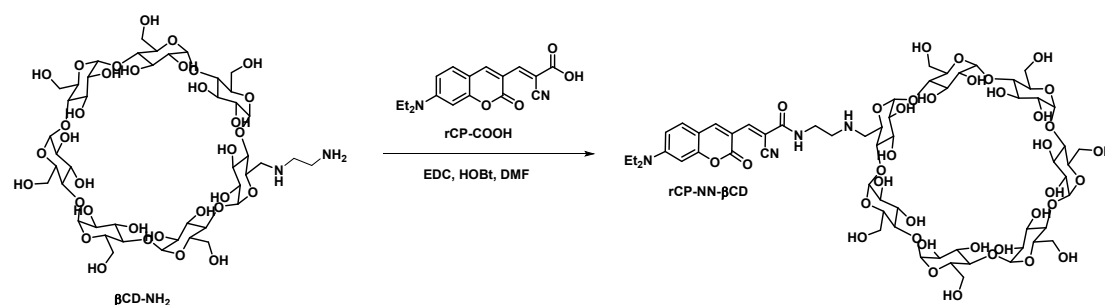
## Table of Contents

1. Experimental .....	2
2. Synthesis .....	2
3. UV-Vis absorption and fluorescence spectroscopy .....	3
4. Cell imaging experiment .....	9
5. Characterization data .....	10
6. References .....	11

## Experimental

All chemicals reagents and solvents for synthesis were purchased from commercial sources (Aladdin Industrial Corporation, Tokyo Chemical Industry and Sigma-Aldrich Chemical) and were used without further purification. Ultrapure water was used after passing through a water ultra-purification system.  $^1\text{H-NMR}$ ,  $^{13}\text{C-NMR}$  spectra were recorded on an Ascend 400 MHz (BRUKER) at room temperature. High-resolution mass spectra (HRMS) were measured on 6520 Q-TOF LC/MS (Agilent). Absorption spectra was recorded on a UV-vis spectrophotometer (UV-2700, Shimadzu), and steady-state fluorescence emission spectra were recorded in a conventional quartz cell ( $10 \times 10 \times 45$  mm) at  $25^\circ\text{C}$  on a Varian Cary Eclipse equipped with a Varin Cary single-cell peltier accessory to control temperature. Absolute fluorescence quantum yields were recorded on a FLS980 instrument (Edinburg Instruments Ltd., Livingstone, UK). CD spectra were recorded on Jasco J 715 CD spectrophotometers. Confocal fluorescence and bright-field imaging were recorded with FV1000 (Olympus).

## Synthesis



**Scheme S1.** Synthesis of **rCP-NN-βCD** and the structure of **rCP-βCD**.

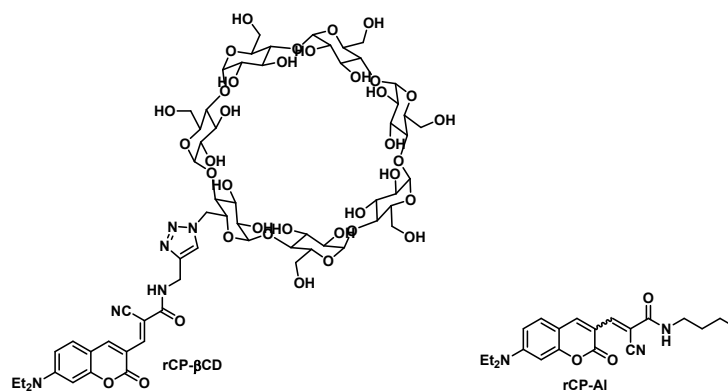
**βCD-NH<sub>2</sub>**: **βCD-NH<sub>2</sub>** was synthesized according to the reported procedure.<sup>1</sup>

**rCP-COOH**: **rCP-COOH** was synthesized according to the reported procedure.<sup>2</sup>

**rCP-NN-βCD**: **rCP-COOH** (400 mg, 1.28 mmol), **EDC** (245.7 mg, 1.28 mmol) and **HOBt** (172.9 mg, 1.28 mmol) were dissolved in anhydrous **DMF** and the solution was stirred at room temperature for 30 min. After that, **βCD-NH<sub>2</sub>** (233.8 mg, 1.07 mmol) was added, and the reaction mixture was stirred overnight. Finally, the solution was evaporated, and the resultant residue was purified by silica gel chromatography to afford **rCP-NN-βCD** (160.9 mg, 66%) as a red solid.

$^1\text{H-NMR}$  (400 MHz, **DMSO**)  $\delta$  8.68 (s, 1H), 8.20 (s, 1H), 8.15 (s, 1H), 7.60 (d,  $J = 9.1$  Hz, 1H), 6.82 (d,  $J = 7.1$  Hz, 1H), 6.64 (s, 1H), 5.88 – 5.49 (m, 14H), 4.85 (m, 7H), 4.47 (d,  $J = 3.9$  Hz, 6H), 3.82 – 3.49 (m, 30H), 2.65 – 2.84 (m, 5H), 1.15 (t,  $J = 7.0$  Hz, 6H).

$^{13}\text{C}$ -NMR (100 MHz, DMSO)  $\delta$  160.20, 157.23, 152.98, 144.25, 143.46, 131.92, 116.69, 110.48, 110.14, 107.78, 102.30, 101.98, 96.54, 83.07, 82.06, 81.55, 81.26, 73.01, 72.38, 71.99, 59.89, 44.53, 12.36.  
 HRMS-ESI (m/z):  $[\text{M}+\text{H}]^+$  calcd for  $\text{C}_{61}\text{H}_{90}\text{N}_4\text{O}_{37}$ : 1471.5284; found: 1471.5362.



**Scheme S2.** The structures of rCP-βCD of rCP-AI.

rCP-βCD and rCP-AI were synthesized according to the reported procedure.<sup>2</sup>

## UV-vis absorption and fluorescence spectroscopy

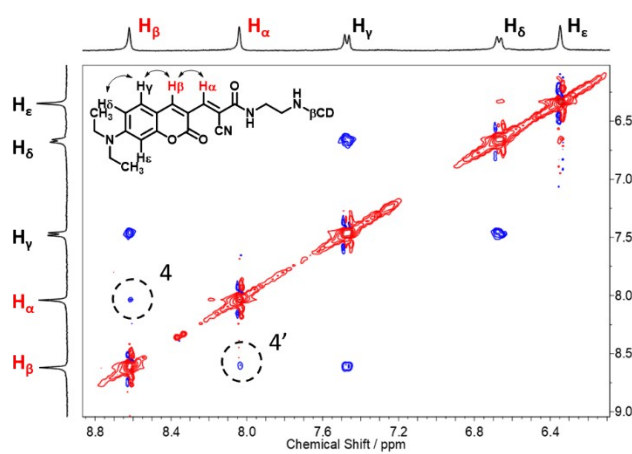


**Figure S1.** Enlarged NMR ROESY spectrum of the coumarin moiety on rCP-NN-βCD (4 mM) in  $\text{D}_2\text{O}$  and the configuration of coumarin (400 MHz).

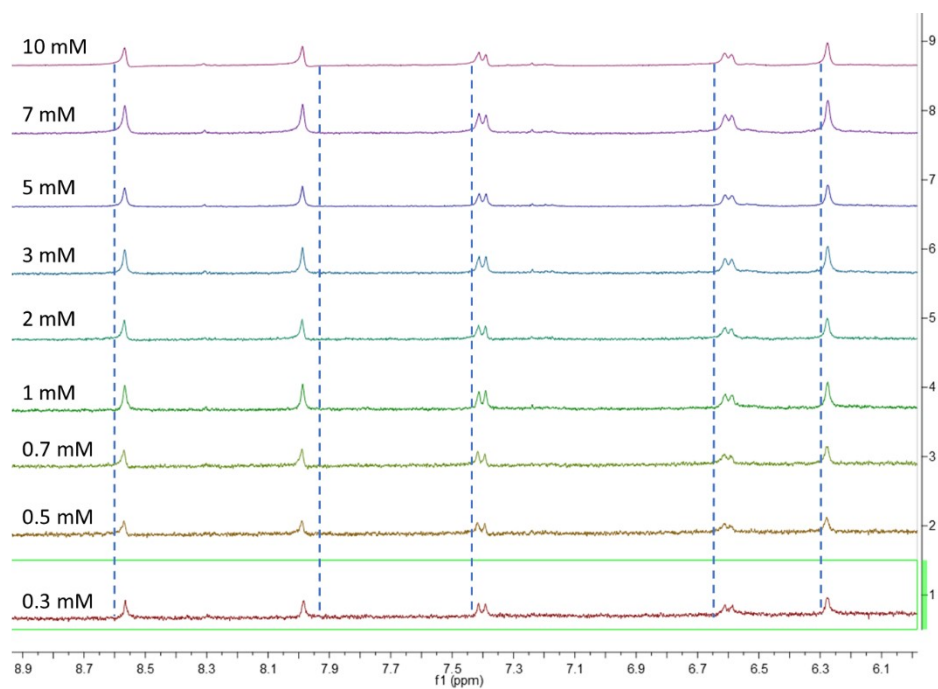


**Figure S2.** <sup>1</sup>H-NMR spectra of rCP-NN-βCD at different concentration in D<sub>2</sub>O (400 MHz).

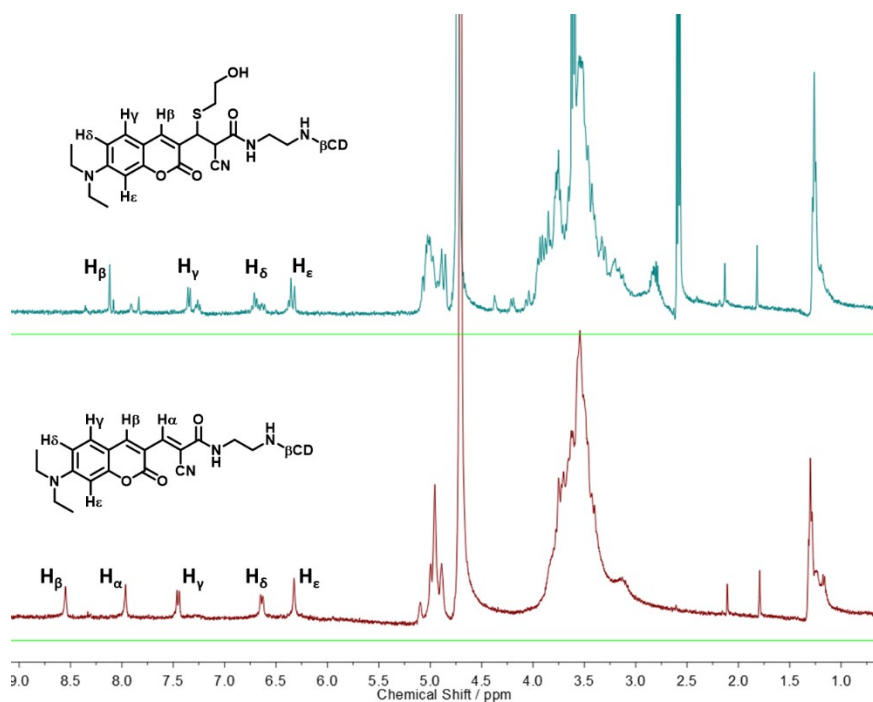


**Figure S3** <sup>1</sup>H-NMR spectra of rCP-NN-βCD (2 mM) and its Michael addition adduct with 2-mercaptoethanol (4 mM) in D<sub>2</sub>O (400 MHz).

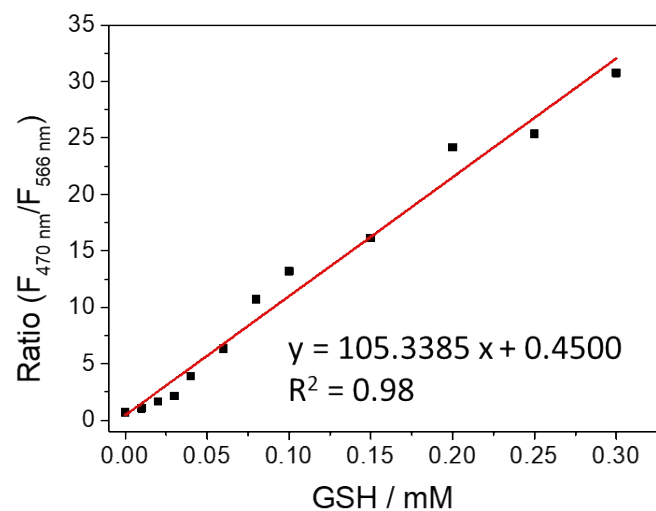


**Figure S4.** The line relationship between the fluorescent intensity ratio of the **rCP-NN-βCD** (10 μM at 470 nm and 566 nm) and the concentration of the GSH in PBS buffer (pH 7.4, 10 mM). Each spectrum was recorded after 5 min. (Ex = 409 nm. Slits: 5/5 nm; Ex = 506 nm. Slits: 5/5 nm)

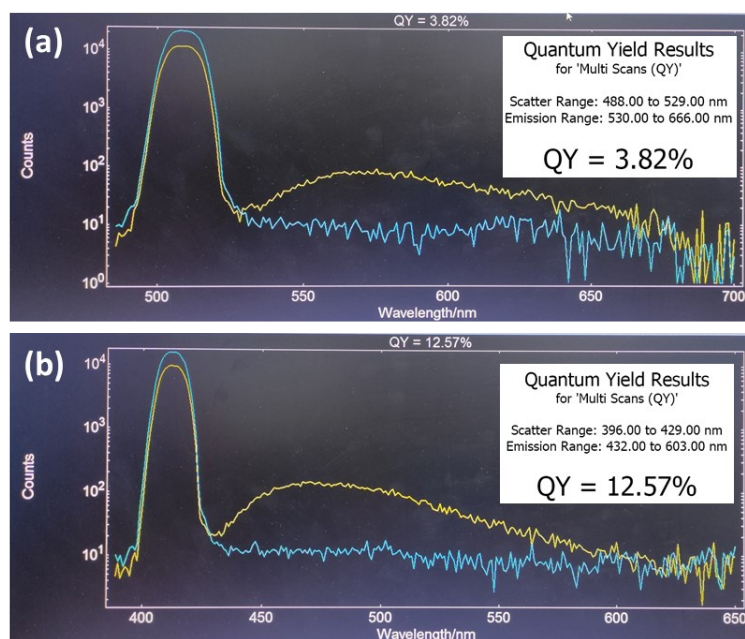


**Figure S5.** Quantum yields of **rCP-NN-βCD** (a) at 566 nm and **rCP-NN-βCD+GSH** (b) at 470 nm in PBS buffer solution.

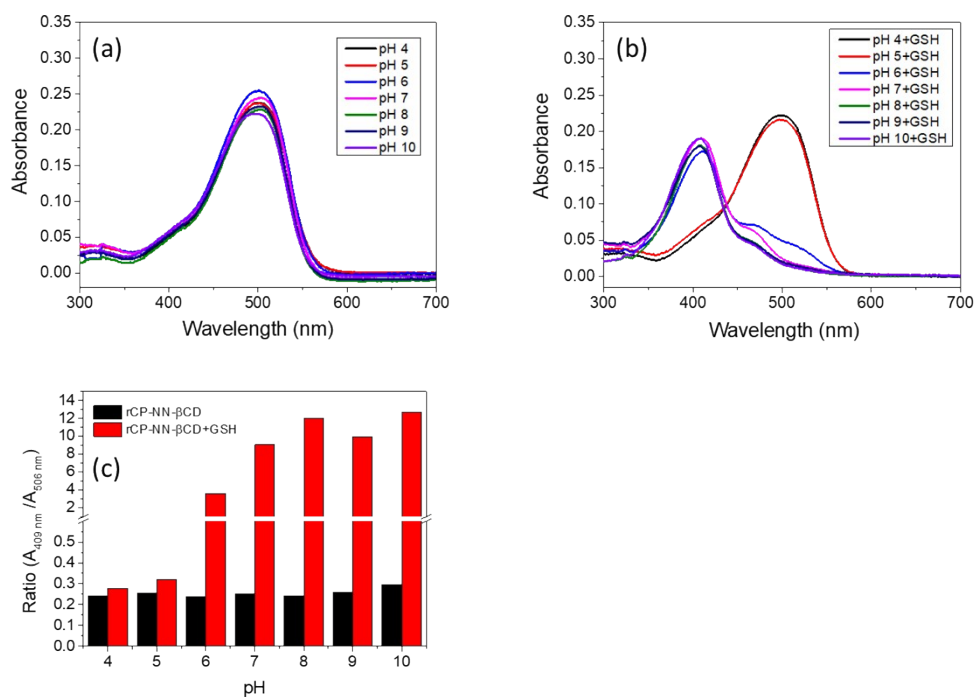


**Figure S6.** UV-vis absorption changes of **rCP-NN-βCD** (10 μM) in the absence or presence of GSH (0.5 mM) in PBS buffer (10 mM) at varied pH values (4 - 10). (a) **rCP-NN-βCD**; (b) **rCP-NN-βCD+GSH**; (c) the ratio (A<sub>409nm</sub>/A<sub>506nm</sub>) of (a) and (b).

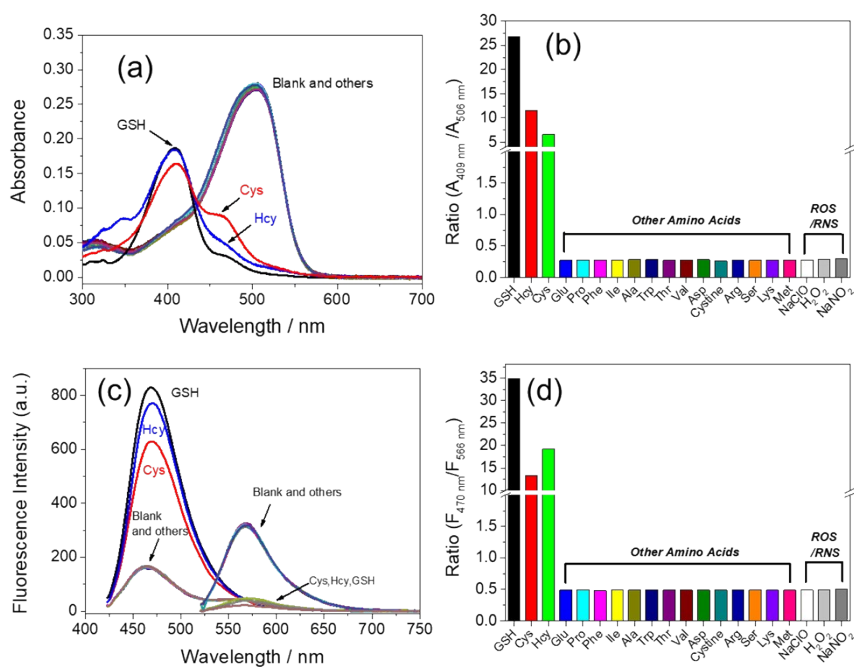


**Figure S7.** UV-Vis absorption and fluorescence response of **rCP-NN-βCD** to intracellular amino acids (0.5 mM), (Cys = Hcy = GSH = 0.5 mM), NaClO (0.1 mM), H<sub>2</sub>O<sub>2</sub> (0.1 mM), NaNO<sub>2</sub> (0.1 mM). (Ex= 409 nm. Slits: 5/5 nm; Ex= 506 nm. Slits: 5/5 nm)

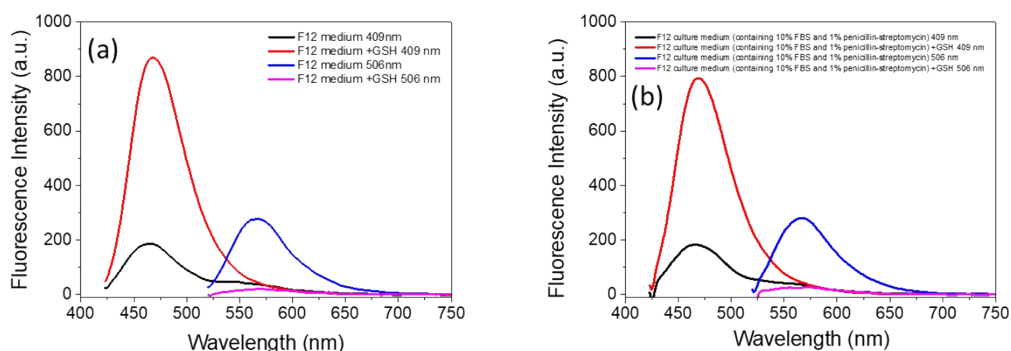


**Figure S8.** The detection performance of **rCP-NN-βCD** toward GSH in F12 culture medium (a) and FBS (b) (containing 10% FBS and 1% penicillin-streptomycin). Fluorescence responses of **rCP-NN-βCD** (10 μM) upon addition of GSH (0.5 mM). (Ex = 409 nm; slits: 5/ 5 nm; Ex = 506 nm; slits: 5/ 5 nm).

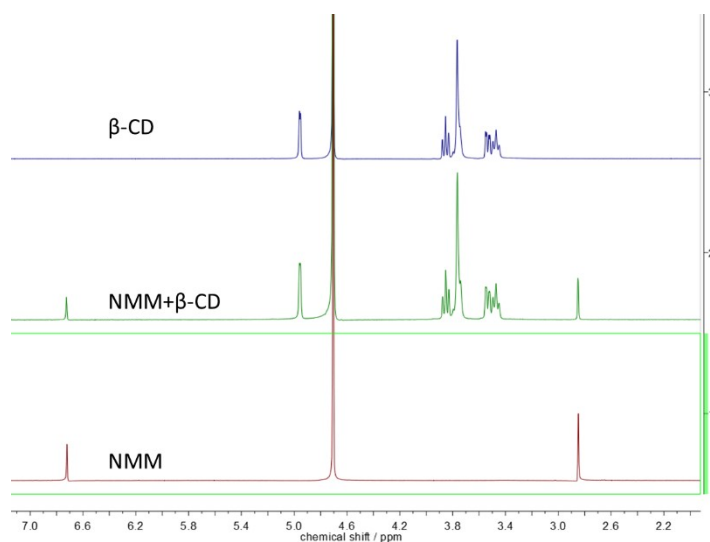


**Figure S9.** <sup>1</sup>H-NMR spectra of NMM (2.5 mM), β-CD (2.5 mM), and NMM+β-CD (1:1) in D<sub>2</sub>O (400 MHz).

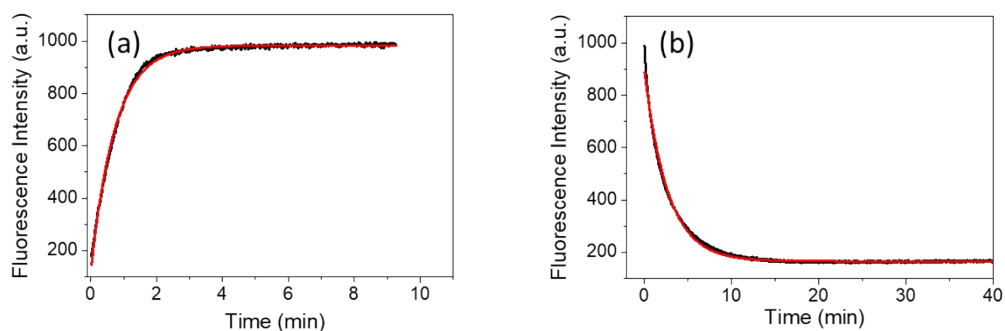


**Figure S10.** Time-dependent fluorescent emission of **rCP-NN-βCD** toward GSH (a) and NMM (b). (Ex = 409 nm; slits: 5/ 5 nm; Em = 470 nm; GSH = 0.5 mM; NMM = 0.5 mM)

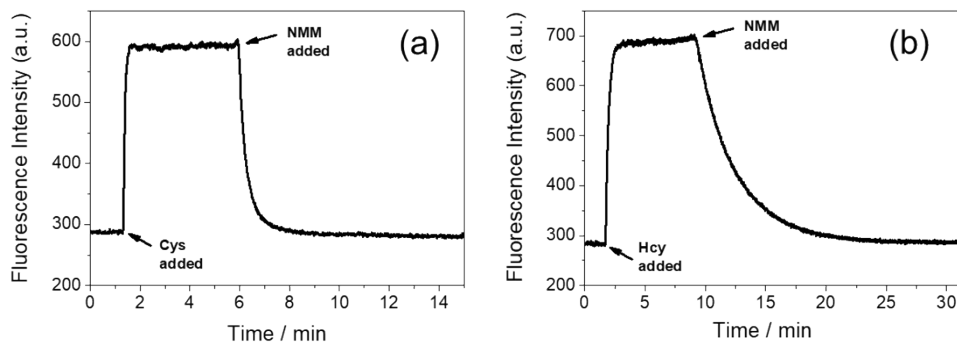


**Figure S11.** Time-dependence reversible fluorescence emission at 470 nm by **rCP-NN-βCD** upon reaction with (a) Cys (0.5 mM) and (b) Hcy (0.5 mM), and then upon addition of NMM (0.5 mM). (Ex = 409 nm. Slits: 5/5 nm)

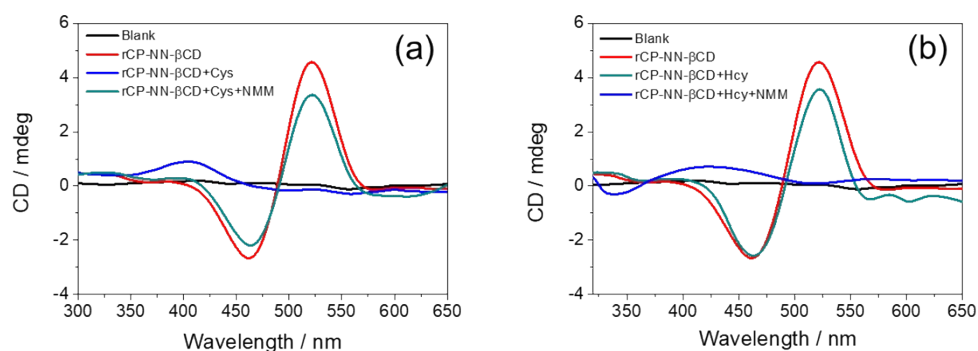


**Figure S12.** Circular dichroism spectra of **rCP-NN-βCD** (10 μM) toward Cys (0.5 mM) and Hcy (0.5 mM), and then upon addition of NMM (0.5 mM).

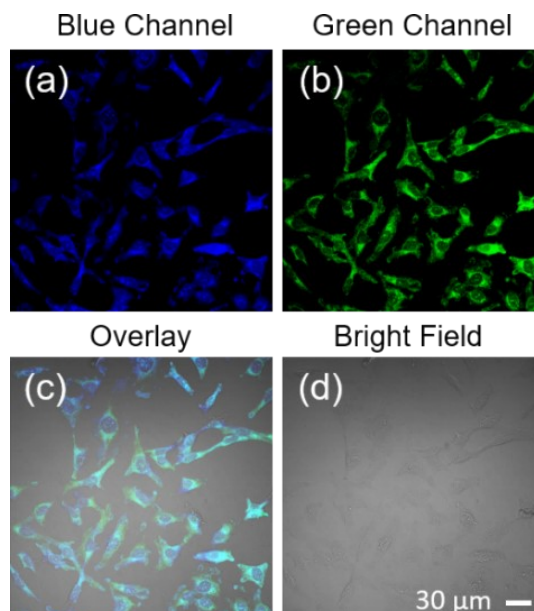


**Figure S13.** Confocal fluorescence images of living HeLa cells incubated with **rCP-NN-βCD** (10 μM). (Blue channel: Excited at 405 nm, Emission was collected at 425-525 nm; Green channel: Excited at 488 nm, Emission was collected at 525-650 nm).



## Cell imaging experiment

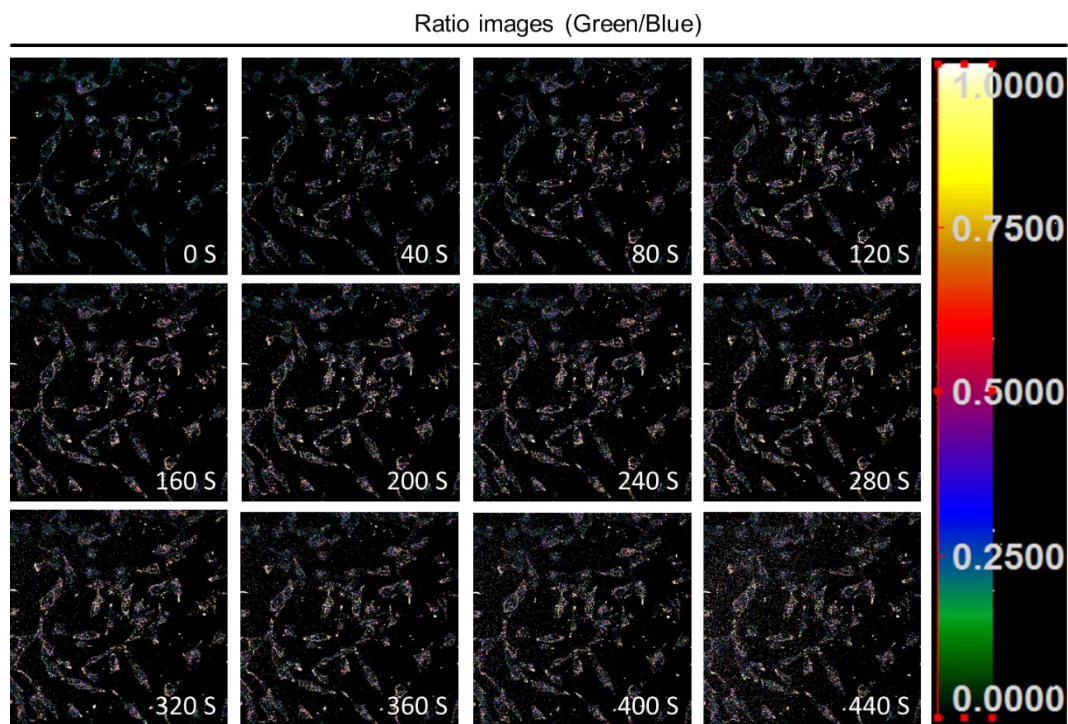


**Figure S14.** Time-dependent ratio (Green/Blue) imaging with **rCP-NN-βCD** (10 μM) in HeLa cells upon addition of NMM (5 mM) within 440 s.

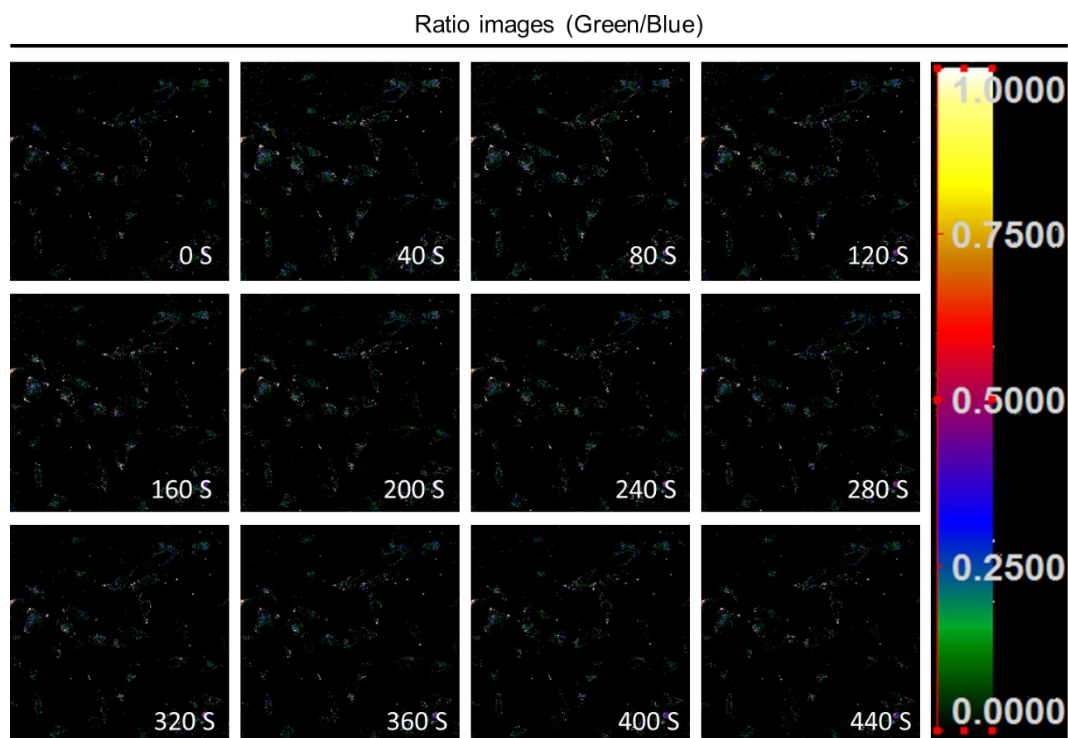


**Figure S15.** Time-dependent ratio (Green/Blue) imaging with **rCP-NN-βCD** (10 μM) in HeLa cells without addition of NMM within 440 s.

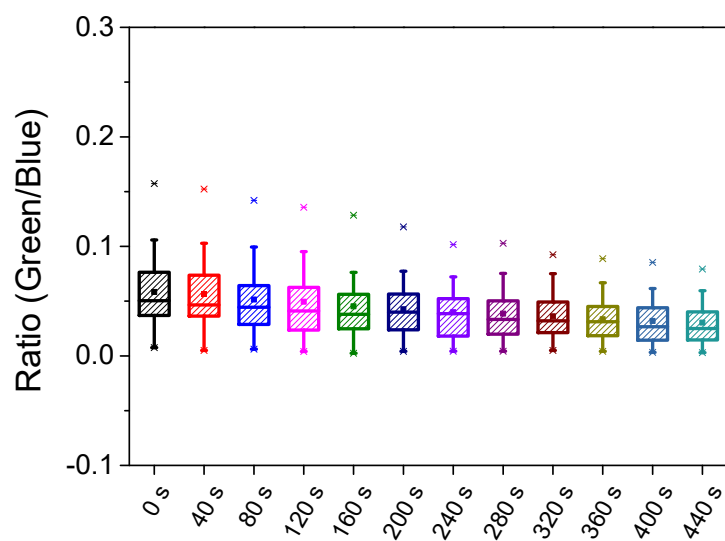


**Figure S16.** Fluorescence quantitative analysis of GSH change in HeLa cells without NMM in individual cells ( $n = 30$ ) for 440 s.

### Characterization data

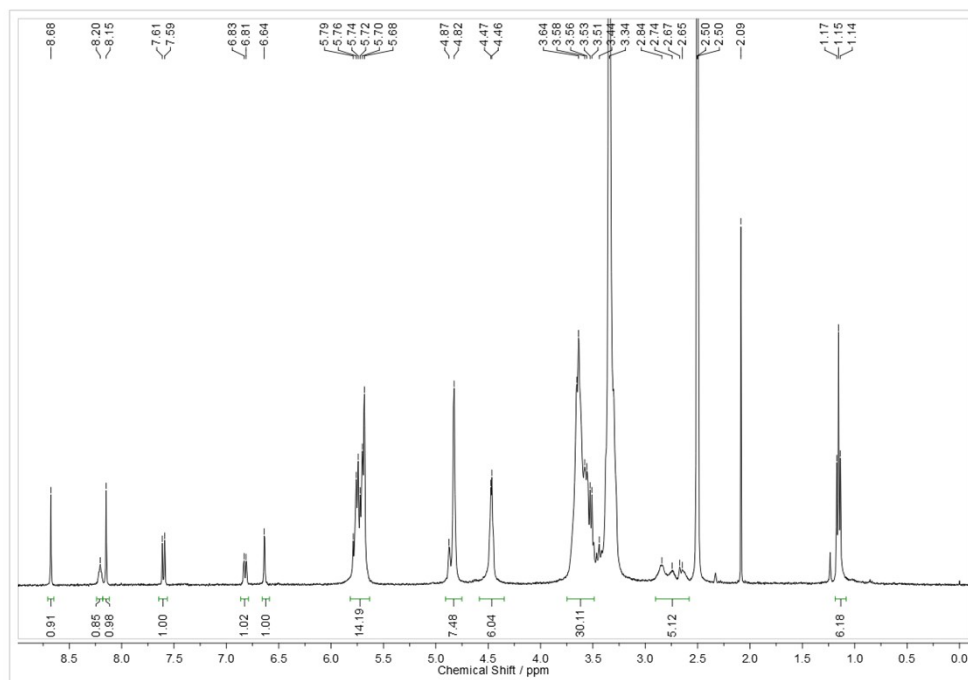


**Figure S17.**  $^1\text{H-NMR}$  spectrum of rCP-NN- $\beta$ CD (400 MHz,  $\text{DMSO-}d_6$ ).

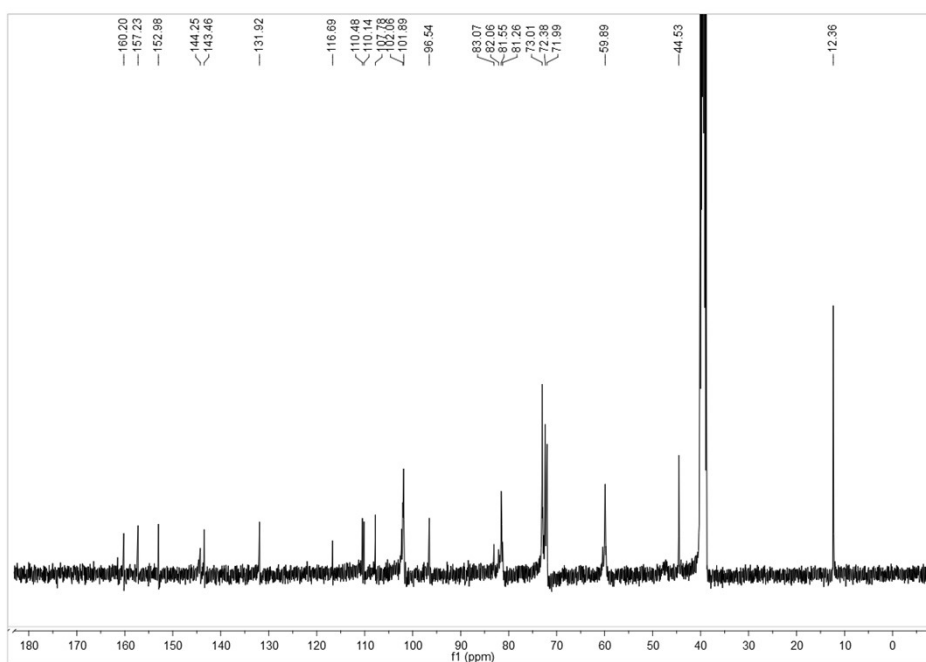


**Figure S18.**  $^{13}\text{C}$ -NMR spectrum of **rCP-NN- $\beta$ CD** (400 MHz,  $\text{DMSO-}d_6$ ).

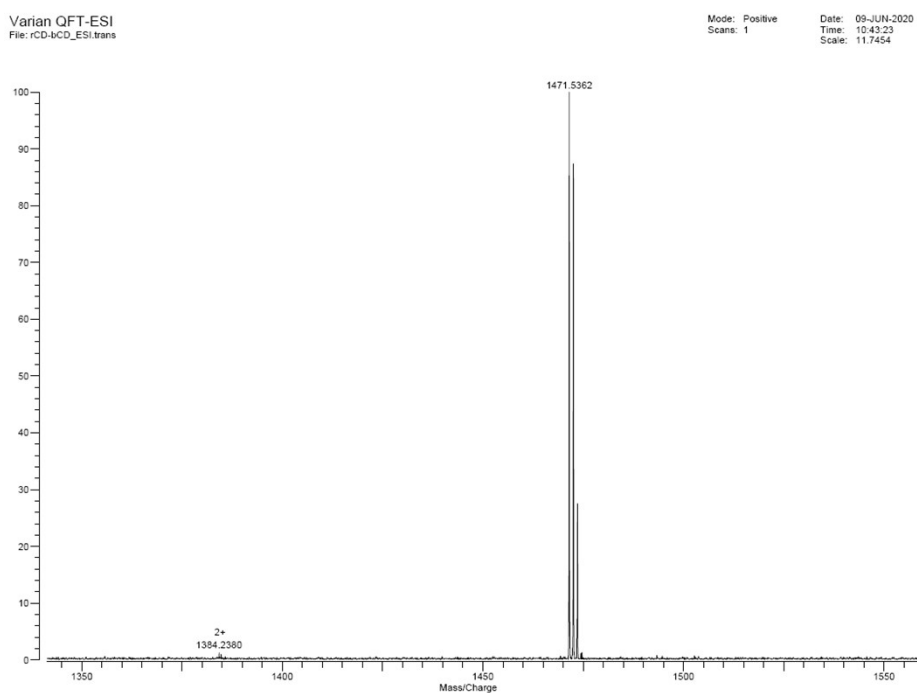


**Figure S19.** HRMS spectrum of **rCP-NN- $\beta$ CD**.

### References:

- Chen, L.; Chen, Y.; Fu, H. G.; Liu, Y., Reversible Emitting Anti-Counterfeiting Ink Prepared by Anthraquinone-Modified beta-Cyclodextrin Supramolecular Polymer. *Adv. Sci.* **2020**, *7*, 2000803.
- Liu, Z.; Zhou, W.; Li, J.; Zhang, H.; Dai, X.; Liu, Y.; Liu, Y., High-efficiency dynamic sensing of biothiols in cancer cells with a fluorescent beta-cyclodextrin supramolecular assembly. *Chem. Sci.* **2020**, *11*, 4791-4800.